

# PROPERTIES OF CHERENKOV DIFFRACTION RADIATION AS PREDICTED BY THE POLARISATION CURRENTS APPROACH FOR BEAM INSTRUMENTATION

D. M. Harryman\*, K. V. Fedorov, P. Karataev

JAI, Royal Holloway, University of London, Egham, Surrey, UK

L. Bobb, Diamond Light Source, Oxfordshire, UK

M. Bergamaschi, R. Kieffer, K. Lasocha, T. Lefevre, S. Mazzoni, A. Schloegelhofer  
CERN, Geneva, Switzerland

A. P. Potylitsyn, Tomsk Polytechnic University, Tomsk, Russia

## Abstract

Cherenkov-Diffraction Radiation (ChDR) appears when a charged particle moves in the vicinity of a dielectric medium with velocity higher than the phase velocity of light inside the medium. As the charged particle does not contact the medium, the emission of ChDR is a phenomenon that can be exploited for a range of non-invasive beam diagnostics. Experimental tests are underway on the Booster To Storage-ring (BTS) test-stand at Diamond Light Source to explore the use of dielectric radiators as Beam Position Monitor (BPM) pickups by measuring the incoherent ChDR emission. In order to compliment the experiments on the BTS test-stand, ChDR simulations have been performed using the Polarisation Currents Approach (PCA) model. This paper explores the PCA simulations for the BTS test-stand, and the application for future diagnostics.

## CHERENKOV DIFFRACTION RADIATION

Cherenkov Diffraction Radiation (ChDR) appears when a charged particle moves in the vicinity of a dielectric medium with velocity higher than the phase velocity of light inside the medium [1]. Detecting ChDR in accelerators is being explored in the development of non-invasive beam diagnostics [2]. ChDR appears at the same distinctive angle as Cherenkov radiation that is given by

$$\cos(\theta_{\text{Ch}}) = \frac{1}{\beta n}, \quad (1)$$

where  $\theta_{\text{Ch}}$  is angle of ChDR emission,  $\beta$  is ratio of the particles velocity compared to the vacuum velocity of light, and  $n$  is the refractive index of the radiator [3,4]. The emission angle of ChDR allows for a detection system to be designed that can discriminate against noise such as synchrotron radiation. A theoretical model to predict the emission of ChDR has been developed in [5–7], the model developed is called the Polarisation Currents Approach (PCA).

## RADIATOR GEOMETRIES

The PCA model can be applied to different radiator geometries where the geometry selected will effect the ChDR

\* daniel.harryman.2018@live.rhul.ac.uk

emission [5, 7]. Figure 1 shows a prismatic ChDR radiator where the notation used is as follows;  $\gamma$  is the Lorentz factor  $\beta$  is ratio of the particles velocity compared to the vacuum velocity of light,  $\lambda$  is the wavelength of the radiation,  $\varepsilon(\lambda)$  is the wavelength dependant permittivity of the prism,  $\theta_{\text{Ch}}$  is the Cherenkov angle,  $a$  is the length of the surface parallel with the electron trajectory,  $\varphi$  is the vertex angle of the prism,  $\delta$  is  $(90^\circ - \varphi)$ ,  $b$  is the impact parameter,  $h$  is the angled impact parameter (where  $b = h \cos(\delta)$ ), and  $\phi$ ,  $\theta$  are respectively the azimuthal and polar angles of the emitted radiation [7].

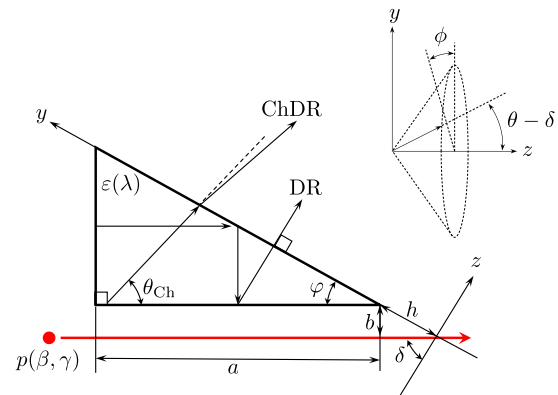


Figure 1: Prismatic Radiator Geometry.

Using a prismatic radiator, the ChDR is generated at the Cherenkov angle which is distinctively different to that of the particle trajectory, once the ChDR reaches the emission surface of the prism it will be emitted at a refracted angle using Snells law [8]. Knowing the index of refraction for the prism, the outside interface, and the Cherenkov angle for that radiator, the vertex angle of the prism is selected for a desired extraction angle. As the ChDR is generated along the entire target length it will be emitted along the majority of the extraction surface.

Extensive work has been done in [7] to obtain the ChDR angular distribution emitted from a prismatic radiator when a charge particle moves parallel to one side (see in Fig. 1). Each polarisation component is then given by Eqs. (2), (3) and (4), where  $\hbar$  denotes the reduced Plank constant,  $\alpha$  is the fine structure constant,  $c$  is the vacuum speed of light, and the notation from Fig. 1 has been used [7].

$$\begin{aligned} \frac{d^2 W_1}{d\lambda d\Omega} = & \frac{\alpha \hbar c \beta^2 \cos^2(\theta - \delta)}{2\pi^2 \lambda^2 K^2 |P|^2} \left| \frac{\varepsilon(\lambda) - 1}{\varepsilon(\lambda)} \right|^2 \times \left| 1 - \exp \left[ -ia \frac{2\pi}{\beta \lambda} (P + \Sigma \cdot \cot(\varphi)) \sin(\varphi) \right] \right. \\ & - \frac{P \exp \left[ i \frac{2\pi}{\beta \lambda} \Sigma \cdot a \cdot \cos(\varphi) \right]}{P + \Sigma \cdot \cot(\varphi)} + \frac{P^2 + \Sigma^2 \cdot \cot^2(\varphi)}{P^2 - \Sigma^2 \cdot \cot^2(\varphi)} \exp \left[ -ia \frac{2\pi}{\beta \lambda} P \cdot \sin(\varphi) \right] \\ & \left. - \frac{\Sigma \cdot \cot(\varphi) \exp \left[ -i \frac{2\pi}{\beta \lambda} \Sigma \cdot a \cdot \cos(\varphi) \right]}{P - \Sigma \cdot \cot(\varphi)} \right|^2 \times \end{aligned} \quad (2)$$

$$\begin{aligned} & \frac{\exp \left[ -\frac{4\pi}{\gamma \beta \lambda} (h + a \cdot \cos(\varphi)) K \cos(\delta) \right]}{1 - \beta^2 \cos^2(\theta - \delta) + \beta^2 \sin^2(\delta) (1 - \sin^2(\theta - \delta) \sin^2(\varphi)) + 2\beta \sin(\delta) \sin(\theta - \delta) \cos(\varphi)} \\ & \times \left| \frac{\varepsilon(\lambda)}{\varepsilon(\lambda) \cos(\theta - \delta) + U} \right|^2 \left| \cos(\delta) (\gamma^{-1} \sin(\theta - \delta) - iKU \cos(\varphi)) + \right. \\ & \left. \sin(\delta) (iK \sin(\theta - \delta) + \gamma^{-1} U \cos(\varphi)) - \gamma \beta U \sin(\theta - \delta) \sin^2(\varphi) \right|^2, \end{aligned}$$

$$\begin{aligned} \frac{d^2 W_2}{d\lambda d\Omega} = & \frac{\alpha \hbar c \beta^2 \cos^2(\theta - \delta)}{2\pi^2 \lambda^2 K^2 |P|^2} \left| \frac{\varepsilon(\lambda) - 1}{\varepsilon(\lambda)} \right|^2 \gamma^2 \sin^2(\varphi) \left| \frac{\sqrt{\varepsilon(\lambda)}}{\cos(\theta - \delta) + U} \right|^2 (\sin^2(\theta - \delta) + |U|^2) \\ & \times \left| 1 - \exp \left[ -ia \frac{2\pi}{\beta \lambda} (P + \Sigma \cdot \cot(\varphi)) \sin(\varphi) \right] - \frac{P \exp \left[ i \frac{2\pi}{\beta \lambda} \Sigma \cdot a \cdot \cos(\varphi) \right]}{P + \Sigma \cdot \cot(\varphi)} \right. \\ & \left. + \frac{P^2 + \Sigma^2 \cdot \cot^2(\varphi)}{P^2 - \Sigma^2 \cdot \cot^2(\varphi)} \exp \left[ -ia \frac{2\pi}{\beta \lambda} P \cdot \sin(\varphi) \right] - \frac{\Sigma \cdot \cot(\varphi) \exp \left[ -i \frac{2\pi}{\beta \lambda} \Sigma \cdot a \cdot \cos(\varphi) \right]}{P - \Sigma \cdot \cot(\varphi)} \right|^2 \times \end{aligned} \quad (3)$$

$$\begin{aligned} & \frac{\exp \left[ -\frac{4\pi}{\gamma \beta \lambda} (h + a \cdot \cos(\varphi)) K \cos(\delta) \right]}{1 - \beta^2 \cos^2(\theta - \delta) + \beta^2 \sin^2(\delta) (1 - \sin^2(\theta - \delta) \sin^2(\varphi)) + 2\beta \sin(\delta) \sin(\theta - \delta) \cos(\varphi)} \\ & \times [1 - \beta^2 \cos^2(\theta - \delta) + 2\beta \gamma^{-2} \sin(\theta - \delta) \cos(\varphi) - \gamma^{-2} \sin^2(\delta) (K^2 - \gamma^{-2})], \end{aligned}$$

$$\begin{aligned} U &= \sqrt{\varepsilon(\lambda) - \sin^2(\theta - \delta)}, \\ P &= \cos(\delta) - \beta U + i\gamma^{-1} K \sin(\delta), \\ \Sigma &= \sin(\delta) + \beta \sin(\theta - \delta) \cos(\varphi) - i\gamma^{-1} K \cos(\delta), \\ K &= \sqrt{1 + (\gamma \beta \sin(\theta - \delta) \sin(\varphi))^2}, \end{aligned} \quad (4)$$

An approximation made in Eqs. (2), (3), and (4) is that the prism is infinite in length in the plane orthogonal to the particle trajectory.

Another type of ChDR radiator is the Accumulator shown in Fig. 2. The benefit of the accumulator ChDR radiator is that the ChDR is accumulated along the length of the radiator. The ChDR is kept inside the target via total internal reflection until it reaches the reflective surface at the end where it is extracted [2,9]. Similar to a prismatic radiator the vertex angle,  $\varphi$  is selected to specify the ChDR extraction angle for an accumulator radiator.

## DIAMOND LIGHT SOURCE BEAM TEST-STAND

Diamond Light Source is a 3<sup>rd</sup> generation synchrotron light source in the U.K. The Diamond accelerator chain consists of three accelerators; a linac, a booster synchrotron, and

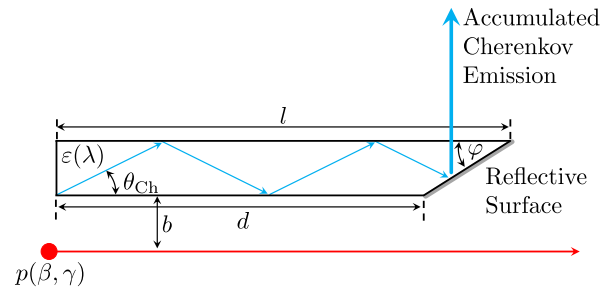


Figure 2: Accumulator Radiator Geometry.

a storage ring. On the Booster to Storage-ring (BTS) transfer line is a beam test-stand available for testing accelerator components and novel diagnostic instrumentation. In recent years a ChDR experimental setup has been installed onto the Diamond beam test-stand in order to examine the properties of incoherent ChDR and its application as a Beam Position Monitor (BPM) pickup [9].

The booster synchrotron can extract through the BTS in two modes, Multi-Bunch extraction or Single-Bunch extraction. Table 1 shows the nominal Single-Bunch extraction beam parameters of the BTS.

The BTS ChDR experiment is fitted with a CVD Diamond accumulator target with a length, of 15 mm and a vertex an-

Table 1: Single-Bunch Extraction Parameters on the Diamond BTS [10]

Standard BTS Parameter	Value
Beam Energy	3 GeV
Horizontal Beam Size $\sigma_x$	1.27 – 1.42 mm
Vertical Beam Size $\sigma_y$	0.57 – 0.6 mm
Extraction Rate	5 Hz
Max Bunch Charge (SBE)	0.2 nC
Bunch Length	$\approx 2.5$ mm

gle, of  $12.5^\circ$ . It is assumed that the angular distributions simulated from a prismatic radiator will have similar angular distributions to those measured from the accumulator radiator as long as the length, vertex angle, and properties of the medium are kept the same.

The ChDR emission is coupled out of the radiator through a viewport into an optical system. The optical system features a polariser and a filter wheel fitted with 0.4 and 0.55  $\mu\text{m}$  bandpass filters [9].

## SIMULATIONS

### Single Particle Simulations

Multiple radiators can be configured in classical BPM configurations, where only a single intensity measurement is needed from each radiator. To obtain an intensity measurement from a ChDR radiator a detector would be placed at the ChDR emission angle of the radiator. The intensity read by the detector would then be proportional to the energy of the emitted radiation. The energy of emitted radiation,  $\Delta W$  in the fixed angular and wavelength intervals,  $\Delta\Omega$  and  $\Delta\lambda$  can be simulated using

$$\Delta W = \int_{\Delta\Omega} d\Omega, \int_{\Delta\lambda} \frac{d^2W}{d\lambda d\Omega} d\lambda, \quad (5)$$

where  $dW$  is the energy emitted per unit of wavelength,  $d\lambda$ , per unit of solid angle,  $d\Omega$  [7]. The solid angle component is given by

$$d\Omega = \sin(\theta)d\theta d\phi, \quad (6)$$

where  $\theta$  is the polar angle of the angular distribution, and  $\phi$  the azimuthal. By producing a series of angular distributions with Eqs. (2), (3), and (4) then integrating each one, parameter dependencies of the emitted ChDR can be calculated.

Figure 3 shows the spectrum of ChDR emitted for a single 3 GeV electron from the ChDR radiator used on the BTS test-stand at Diamond for range of impact parameters.

The spectrum for the 1 and 100  $\mu\text{m}$  impact parameters in Fig. 3 follow the Cherenkov dependence of  $1/\lambda$ . As the impact parameter is increased the ChDR intensity drops, across all wavelengths but dramatically more at shorter wavelengths resulting in a peak appearing when

$$b \approx \frac{\gamma\lambda}{2\pi}, \quad (7)$$

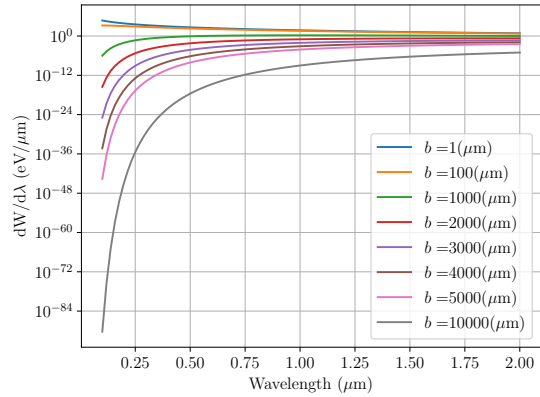


Figure 3: Single particle ChDR spectral emission at a range of impact parameters,  $b$ , from the ChDR radiator installed on the BTS test-stand.

as this is the edge of the pre-wave zone [11]. Figure 4 shows the impact parameter dependence for a single particle and the setup on BTS test-stand at fixed wavelengths. At impact parameters of  $< 500 \mu\text{m}$  the short wavelength of  $0.4 \mu\text{m}$  dominates, beyond this limit the longer wavelength of  $0.55 \mu\text{m}$  does. This effect continues for all wavelengths, for a ChDR BPM with a working impact parameter region of at least several millimetres an optical system in the infrared region would be better suited. Using the same theory a ChDR beam halo monitor would require an optical detection system sensitive to shorter wavelengths to dampen the signal from the core of the beam.

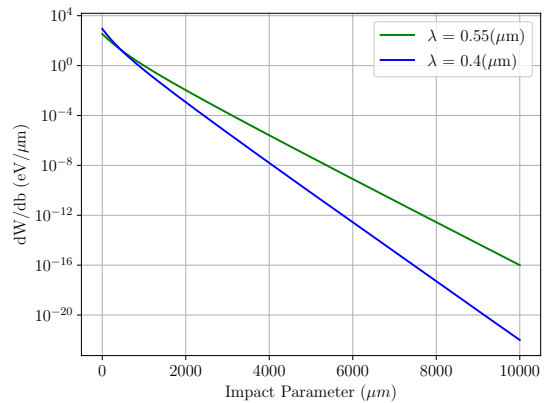


Figure 4: ChDR impact parameter dependence at fixed wavelengths from the ChDR radiator installed on the BTS test-stand from a single 3 GeV electron.

### Beam Distribution Simulations

In order to simulate angular distributions for a beam profile the single particle angular distributions are calculated using Eqs. (2), (3) and (4) at each impact parameter then scaled by the bunch charge at that impact parameter. The

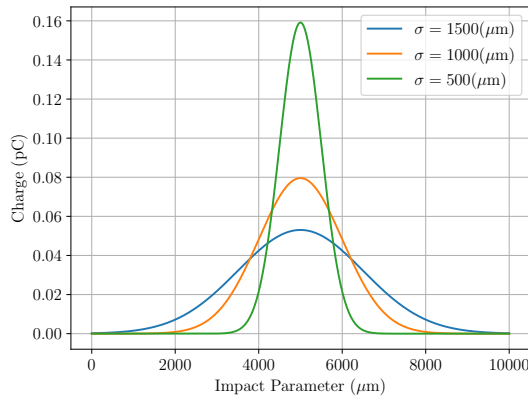


Figure 5: Horizontal transverse beam distributions centred at an impact parameter of 5 mm with a charge of  $\approx 0.2$  nC each.

simulations in this paper only consider a horizontal beam profile due to the infinite length assumed in Eqs. (2), (3) and (4).

Initial testing on the BTS has shown that the horizontal beam size can be changed between  $\approx 0.5$  to 1.5 mm. Figure 5 shows three different horizontal beam profiles centred at an impact parameter of 5 mm each profile considers a bunch charge of 0.2 nC.

In order to verify the PCA model when extended to a multi-electron beam the predicted angular distributions and dependency scans must be compared to experimental data. Particles that directly collide with the radiator will generate Cherenkov radiation that will be measured by the optical system introducing noise into the measurements. The PCA model shows the spectral dependence of Cherenkov radiation and ChDR are different so long as the impact parameter is sufficiently large (see Fig. 3). To confirm the PCA model it is beneficial to work in a regime where the ChDR spectral response does not follow that of Cherenkov radiation.

By performing an element wise multiplication between transverse beam distributions and impact parameter dependencies shown in Fig. 5 and 4 respectively the intensity contribution at each impact parameter from the respective beam distribution is produced (see Fig. 6).

Figure 6 shows the horizontal beam size of 1000 and 1500  $\mu\text{m}$  result in a signal that is dominated by the edge of the beam profile located at low impact parameters. This is of concern as particles at impact parameters close to the radiator produce a spectrum that appears as the Cherenkov spectrum (see Fig. 3).

Figure 7 shows the effect of horizontal beam size on ChDR emission intensity for a beam centred at an impact parameter of 5000  $\mu\text{m}$ . The smaller the horizontal beam size the more the signal becomes dominated by the core of the beam resulting in an emission dominated by longer wavelengths. Conversely as the beam size gets larger the signal becomes

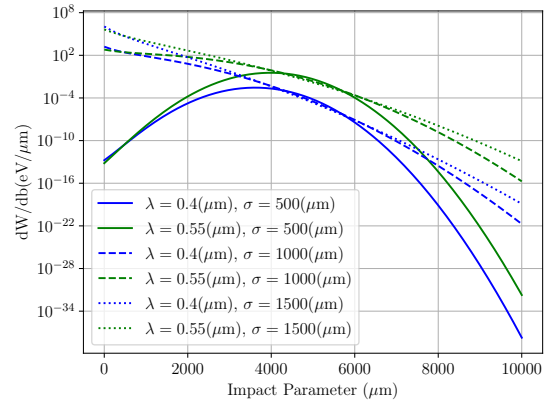


Figure 6: Signal contribution at each impact parameter emitted from the BTS ChDR radiator from the beam distributions in Fig. 5.

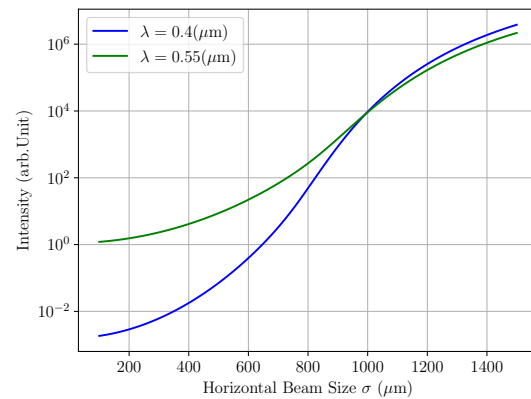


Figure 7: Effect of horizontal beam size from a beam at centred at an impact parameter of 5000  $\mu\text{m}$  on ChDR intensity yield from the radiator on the BTS test-stand.

dominated by the edge of the distribution near the radiator favouring the signal from the shorter wavelengths.

## CONCLUSION

This paper presents simulations of ChDR emission for the BTS test-stand at Diamond Light Source using the PCA model. It has been found that ChDR emission at longer wavelengths is most sensitive to the core of the beam, whereas shorter wavelengths are dominated by the particles in the beam tails. For BPM applications, an infrared system is most suitable whereas a beam halo monitor could be developed using the ChDR emission in the visible range.

Future steps for this research will compare the angular distributions measured from the optical system on the BTS test-stand with those simulated. Differences are expected between the simulations and measurements due to the different radiator geometries used in each. More in-depth and useful experiments would compare the spectral emission and impact parameter dependences.

## REFERENCES

- [1] R. Kieffer, *et al.* “Direct observation of incoherent Cherenkov diffraction radiation in the visible range”, *Phys. Rev. Lett.*, vol. 121, p. 054802, Aug 2018. doi:10.1103/PhysRevLett.121.054802
- [2] T. Lefèvre *et al.*, “Cherenkov Diffraction Radiation as a tool for beam diagnostics”, in *Proc. IBIC'19*, Malmö, Sweden, Sep. 2019, pp. 660–664. doi:10.18429/JACoW-IBIC2019-THA001
- [3] P.A. Cerenkov, “Visible radiation produced by electrons moving in a medium with velocities exceeding that of light”, *Phys. Rev.*, vol. 52, pp. 378–379, Aug 1937. doi:10.1103/PhysRev.52.378
- [4] I. Tamm, “Radiation emitted by uniformly moving electrons”, *Journal of Physics (USSR)* vol. 1, pp. 439–454, 1937.
- [5] M. V. Shevelev and A. S. Konkov, “Peculiarities of the generation of Vavilov-Cherenkov radiation induced by a charged particle moving past a dielectric target”, *Journal of Experimental and Theoretical Physics*, vol. 118, no. 4, pp. 501–511, Apr. 2014. doi:10.1134/S1063776114030182
- [6] D. V. Karlovets and A. P. Potylitsyn, “Universal description for different types of polarization radiation”, Aug. 2009. arXiv:0908.2336
- [7] A. S. Konkov, J. S. Markova, A. P. Potylitsyn, V. V. Bleko, V.V. Soboleva, and P. V. Karataev, “Theoretical model for incoherent Cherenkov diffraction radiation Report II”, Tomsk Polytechnic University Internal Report, Apr. 2018.
- [8] E. Hecht, “Optics, Global Edition”, Pearson Education Limited, 2016, pp. 109, 170–173.
- [9] D. M. Harryman *et al.*, “First Measurements of Cherenkov-Diffraction Radiation at Diamond Light Source”, in *Proc. IBIC'19*, Malmö, Sweden, Sep. 2019, pp. 624–628. doi:10.18429/JACoW-IBIC2019-WEPP037
- [10] L. Bobb, “Parameters for Experimental Proposals in Booster-to-Storage Ring (BTS) test-stand at Diamond Light Source”, Diamond Light Source, May 2017, unpublished.
- [11] P. V. Karataev, “Pre-wave zone effect in transition and diffraction radiation: Problems and solutions”, *Physics Letters A*, vol. 345, no. 4, pp. 428–438, 2005. doi:10.1016/j.physleta.2005.07.027